Gene Expression, Vol. 19, pp. 1–13
Printed in the USA.

1052-2166/19 $90.00 + .00
DOI: https://doi.org/10.3727/105221618X15293258688953
E-ISSN 1555-3884
www.cognizantcommunication.com

Hepatic Gene Expression During the Perinatal Transition in the Rat

Edward Hurley,*† Valerie Zabala,*‡ Joan M. Boylan,*‡
Philip A. Gruppuso,*‡§ and Jennifer A. Sanders*‡¶

*Department of Pediatrics, Brown University, Providence, RI, USA
†Division of Neonatology, Women and Infants Hospital of Rhode Island, Providence, RI, USA
‡Division of Pediatric Endocrinology, Rhode Island Hospital, Providence, RI, USA
§Department of Molecular Biology, Cell Biology, and Biochemistry, Brown University, Providence, RI, USA
¶Department of Pathology and Laboratory Medicine, Brown University, Providence, RI, USA

During the immediate postnatal (PN) period, the liver, with its role in energy metabolism and macromolecule synthesis, plays a central role in the perinatal transition. Using RNA microarrays and several complementary computational analyses, we characterized changes in hepatic gene expression in the rat across a developmental period starting with the late gestation fetus (embryonic day 21), and including 30 min PN, 4 h PN, 12 h PN, 1 day PN, and 1 week after birth. Following subtle changes in gene expression at the earliest PN time point, there were marked changes that occurred between 4 and 12 h after birth. These reflected changes in multiple metabolic pathways, with expression of enzymes involved in glycolysis and cholesterol synthesis showing the greatest change. Over 50% of nuclear-encoded mitochondrial genes changed in the first 7 days of PN life, with 25% changing within the first 24 h. We also observed changes coinciding with a transient period of synchronous hepatocyte proliferation that we had observed previously, which occurs during the first PN week. Analysis for upstream regulators of gene expression indicated multiple initiating factors, including cell stress, hormones, and cytokines. Also implicated were multiple canonical transcription factor networks. We conclude that changes in gene expression during the early phases of the perinatal transition involve a complex, choreographed network of signaling pathways that respond to a variety of environmental stimuli. This transcriptomic response during the immediate PN period reflects a complex metabolic adaptive response that incorporates a panoply of signaling pathways and transcriptional regulators.

Key words: Liver; Gene expression; Gene ontology; Transcription factors; Metabolism

INTRODUCTION

As the fetus transitions to postnatal (PN) life, the liver, with its dominant role in energy homeostasis, macromolecule synthesis, digestion, and other physiological functions, serves as a meaningful lens through which we can view perinatal events. Much of what we know about perinatal metabolic physiology has been elucidated by examining how specific enzymes, hormones, and signaling pathways change around the time of birth. These studies, often undertaken in laboratory rats, mice, and sheep, have most often focused on the assessment of enzyme abundance or catalytic activity, or mRNA levels of specific metabolic participants and regulators just before and after birth[1–3]. Other studies have measured macromolecules, such as cholesterol, or assessed organelle abundance or function, such as those studies focusing on mitochondrial biology[4,5].

The liver plays a primary role in a variety of essential metabolic and synthetic functions, including drug metabolism, nutrient regulation, carbohydrate metabolism, and production of serum and clotting factors. Many environmental stressors, such as changes in oxygen tension, nutrient availability, and the hormonal milieu, play a role in the transition from fetal to PN life[6,7]. During this timeframe, significant changes occur in the expression of critical genes involved in the essential metabolic functions of the liver, including isoform switching in key genes regulating glycolysis and xenobiotic metabolism[8]. The present studies represent an extension of our longstanding interest in the biology of late gestation fetal rat hepatocytes[9]. We have shown that these cells, like many transformed cell lines, are resistant to the growth inhibitory effects of the mTOR inhibitor, rapamycin, while adult rat hepatocytes are highly sensitive[10]. In fact, our

Address correspondence to Jennifer A. Sanders, Ph.D., Division of Pediatric Endocrinology, Rhode Island Hospital, 593 Eddy Street, Providence, RI 02903, USA. E-mail: Jennifer_Sanders@brown.edu

studies indicate that profound changes in cell signaling, including the coupling of insulin signaling[11] and of the Ras–Raf–MEK–Erk pathway[12], occur during the first PN week. We have also demonstrated that hepatocytes late in gestation in the rat undergo progressive but transient growth arrest just before birth and that term hepatocytes synchronously reenter the cell cycle in the first 2 days of life[13]. By the end of the first week of life, these cells are again quiescent, having adopted a mature hepatocyte phenotype.

Our goal for the present studies was to assess perinatal changes in liver biology in a broad context by focusing on the transcriptome and, using a computational approach, the array of regulatory pathways that are likely involved in perinatal metabolic adaptation. Using the laboratory rat as a model system and analysis by RNA microarray, we studied the period immediately following birth. We anticipated acute changes in gene expression between 30 min and 4 h after birth as pups adapt to postuterine life. We also examined changes in nuclear-encoded mitochondrial genes that occur during this transition to serve as a complement to previously identified postbirth changes in mitochondrial structure and function[5,14,15].

MATERIALS AND METHODS

Animals

Timed pregnant Sprague Dawley rats were obtained from Charles River (Wilmington, MA, USA). Females (8–10 weeks old) were bred with 10- to 12-week-old males. The timed pregnant dams were housed singly upon arrival with ad lib access to water and standard lab chow (Teklad 18% rodent diet; Envigo, East Millstone, NJ, USA). Rodents were maintained on a 12-h on/off light cycle and received standard care including environmental enrichment (hut, wood gnawing blocks, and paper twists). Dams were monitored continuously so the time of birth could be accurately determined. Pups were harvested at the following PN time points: 30 min, 4 h, 12 h, 1 day, and 7 days after birth. They were euthanized by decapitation, and a thoracotomy/laparotomy was performed to access the liver. The livers were flash frozen in liquid nitrogen and then stored at −70°C. To obtain fetal samples at embryonic day 21 (E21), term being 21.5 days, dams were anesthetized using inhaled isoflurane and cesarian sections were performed. Fetuses were externalized one at a time and quickly decapitated before they could draw a breath. A maximum of four fetuses were harvested from each litter so as to avoid excess physiological stress associated with pups delivered late in the cesarian procedure. Fetal livers were harvested and processed in a manner similar to that for PN samples. This study was approved by the Institutional Animal Care and Use Committee of Rhode Island Hospital.

Generation of Transcriptome Data

Pooled E21 fetal liver from a single dam was considered $n = 1$. RNA was extracted from pooled E21 fetal livers from three separate dams and from single pups from three different litters for each PN time point using the RNeasy Mini Kit (QIAGEN, Inc., Germantown, MD, USA) according to the manufacturer's instructions. RNA concentration was measured using a NanoDrop Spectrophotometer (Thermo Fisher Scientific, Waltham, MA). RNA (100 ng) was processed for array using the Affymetrix WT Plus Amplification Kit and Hybridization, Wash, and Stain Kit (Affymetrix, Inc., Sunnyvale, CA, USA). The purity of the RNA was checked with a Bioanalyzer (Agilent, Santa Clara, CA). The Brown University Genomics core laboratory performed the microarray analyses using Rat Transcriptome Assay 1.0 chips (Affymetrix, Inc.). Results were visualized with an Affymetric 3000 7G scanner. All microarray data are available through GEO Series accession number GSE113726 (Private Reviewer Link: https://www.ncbi.nlm.nih.gov/geo/query/acc.cgi?acc=GSE113726). Triplicate arrays were analyzed for each time point.

Microarray Data Analysis

Microarray data were normalized by robust multivariate analysis (RMA) using the Affymetrix Expression Console. The normalized data were filtered to generate a dataset containing all probesets for coding genes. This dataset was used for principal component analysis (PCA) and gene set enrichment analysis (GSEA). One-way ANOVA, pairwise analyses, and generation of volcano plots were performed in R as previously described[16]; the dataset was filtered further using a threshold interquartile range (IQR) of 50%. IQR was performed using the *genefilter* package in Bioconductor[17].

Individual probes that changed significantly [false discovery rate (FDR) p value (q value) of <0.05] across the full-time course, identified using one-way ANOVA, were further analyzed to identify clusters of genes with distinct temporal patterns of expression. To do this, we performed hierarchical clustering by row using Morpheus (https://software.broadinstitute.org/morpheus; Broad Institute, Cambridge, MA, USA). Genes in each cluster were entered into the Ingenuity Pathway Analysis (IPA®; Qiagen Bioinformatics, Redwood City, CA, USA). IPA output consisted of both pathways and upstream regulators associated with changes in gene expression. For IPA results, the threshold for significance was set at $p < 10^{-7}$. This was based on prior analyses of random gene sets[18] and the performance of multiple comparisons in our analyses. A broad range of biologic molecules is listed under "upstream regulators" in IPA including microRNAs, cytokines, and growth factors in addition to traditional

transcription factors. Where noted, we selectively focused on transcription factors.

Pairwise analyses compared individual PN time points with E21. Significance was defined as genes with $q<0.05$ in order to correct for multiple comparisons. Significant genes from this analysis were also subjected to IPA, as described above.

A complementary approach to identify biological pathways associated with changes in gene expression used GSEA (Broad Institute). This method allows for the identification of small changes in sets of functionally related genes[19]. Data were analyzed using both the KEGG and the Reactome suite of pathways. We applied a stringent threshold for significance, $q<0.005$, to account for multiple pairwise comparisons. The relatedness of pathways identified by GSEA was analyzed using Cytoscape[20]. This open source platform graphically depicts networks of pathways that are identified based on genes these pathways have in common.

We conducted separate analyses of nuclear-encoded mitochondrial genes by extracting genes from our dataset that are included in MitoCarta[21]. Significant ($q<0.05$) mitochondrial genes were identified by one-way ANOVA across all time points. These genes were clustered by row using Morpheus (https://software.broadinstitute.org/morpheus). Clusters containing a minimum of 100 genes were used for IPA. Finally, we assessed gene expression changes within specific metabolic pathways. The genes associated with these pathways were identified using PathCards[22], a consolidated compendium of human biological pathways, then analyzed by generating heat maps using Morpheus. Full results from all gene expression analyses are available by correspondence with the authors.

RESULTS

Data Overview

To assess the consistency of gene expression both within time point replicates and across time points, we examined the data using PCA and hierarchical clustering. The PCA plot of the first three components (Fig. 1A) showed that all probesets for coding genes clustered into three distinct groups: E21 fetal/30 min PN/4 h PN, 12 h PN/1 day PN, and 7 days PN. Hierarchical clustering using the 20% most variable probesets for coding genes was (Fig. 1B) consistent with the patterns in the PCA

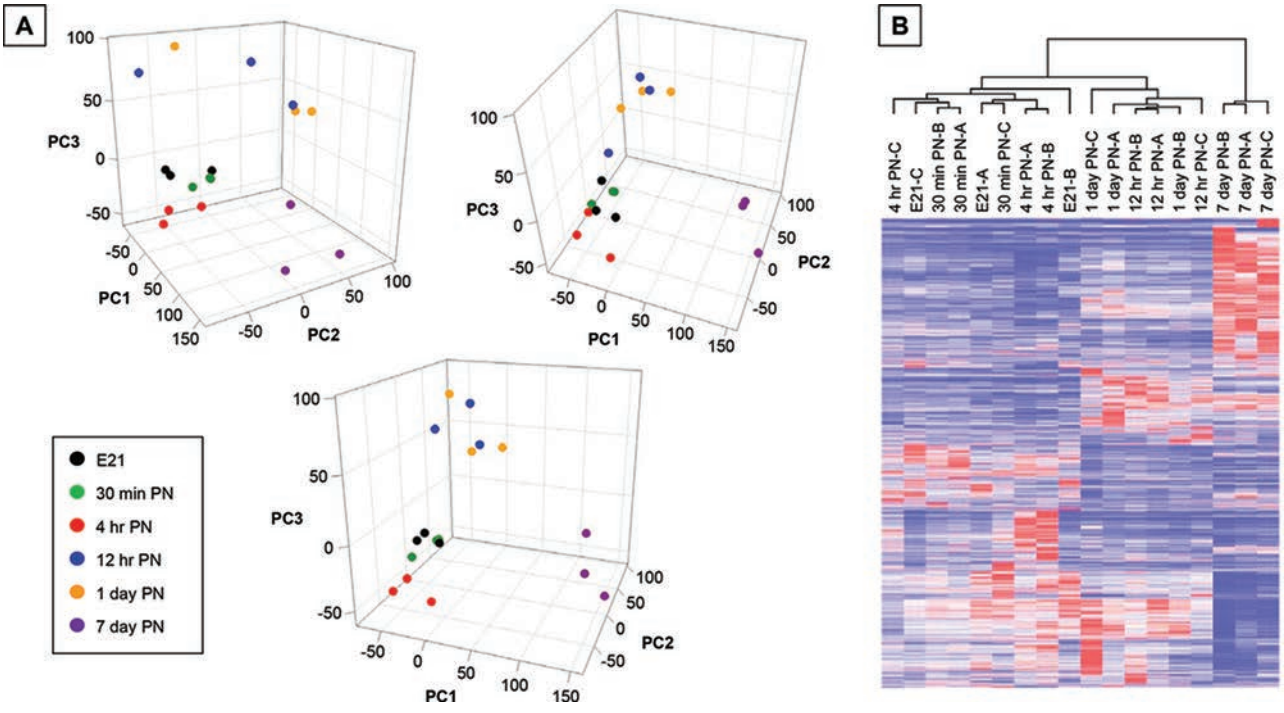

Figure 1. Principal component analysis (PCA) and heat maps/hierarchical clustering of microarray results. (A) PCA was performed using all coding genes from all time points ranging from fetal (embryonic day 21) through 7 days postnatal (PN). The first, second, and third components (PC1, PC2, and PC3) represent 19.7%, 14%, and 10.1% of the variance in the data, respectively. (B) The coefficient of variation (COV) was calculated across all coding samples. The most variable genes (the 20% with the highest COV) were selected for this analysis. Genes were stratified by row. The dendrogram denotes individual samples. The heat map colors represent the relative expression level, with blue corresponding to the lowest level across a row and red corresponding to the highest expression level in that row.

plot. The 7-day PN group showed the greatest segregation from other groups, largely due to an increase in gene expression relative to all other time points. The intermediate time points, 12 h PN and 1 day PN, formed a separate cluster. We interpreted the PCA and clustering results as indicating that there was greater variation between time points than within time points and that there were major transitions that occurred at 4 to 12 h, and beyond 24 h.

Temporal Changes in Postnatal Gene Expression

Genes identified as significant ($q < 0.05$) based on ANOVA were clustered by row. Distinct temporal patterns were most apparent when the approximately 6,500 genes were segregated into 21 clusters. Of these, 12 clusters had fewer than 100 genes and were not analyzed further. IPA was performed on the remaining nine clusters (Fig. 2). The largest cluster, cluster 1, contained genes whose expression was downregulated at 7 days PN compared to the other time points. IPA canonical pathways for this cluster were associated with cell cycle, chromosome replication, protein translation, and mTOR signaling. Transcription factors with well-known roles in the expression of cell cycle regulators and proteins involved in protein synthesis, including c-Myc, E2F family members, and p53, were identified.

There was a subset of genes whose expression was upregulated at 4 h PN (cluster 3) compared to all other time points. Cholecystokinin/gastrin-mediated signaling was the only significant pathway identified for this cluster. The genes accounting for this pathway were immediate early genes (FOS, JUN, and IL1RN), as well as genes involved in cAMP signaling (CREM, ITPR1, and ATF2) and stress signaling (MAPK8, PRKCE, and PRKCH). IPA results for upstream regulators included transcription factors linked to oxidative stress, cytokine, and insulin signaling (NFKB, STAT3, FOXO1, and FOXO3).

Clusters 2 and 5 both showed a transition from 4 to 12 h PN. Cluster 2 contained genes whose expression was downregulated during this timeframe, while cluster 5 contained genes whose expression was upregulated (Fig. 2). No statistically significant canonical pathways were identified for either cluster. However, sterol regulatory

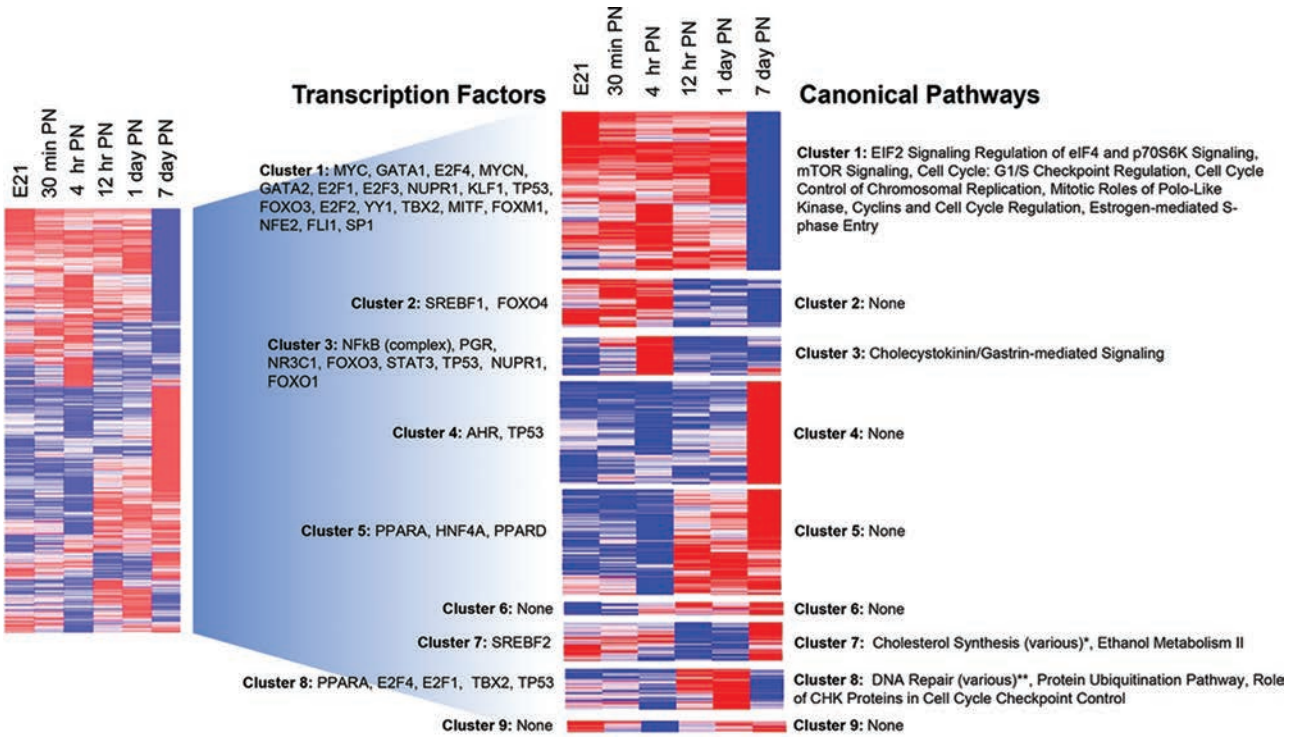

Figure 2. Cluster analysis of the temporal pattern of gene expression. Significant genes ($q < 0.05$), numbering approximately 6,500, were clustered by row. When distinct temporal patterns emerged, the genes formed 21 clusters of which 12 clusters had fewer than 100 genes. These were not subjected to further analysis. The individual genes in each of the remaining nine clusters were entered into the Ingenuity Pathway Analysis (IPA). Significant IPA transcription factors and canonical pathways are shown with clusters numbered from 1 to 9 starting at the top cluster. The heat map colors represent the relative expression level, with blue corresponding to the lowest level across a row and red corresponding to the highest expression in that row. *Cholesterol biosynthesis I, cholesterol biosynthesis II (via 24,25-dihydrolanosterol), cholesterol biosynthesis III (via desmosterol), superpathway of cholesterol biosynthesis. **DNA double-strand break repair by homologous recombination, hereditary breast cancer signaling, ATM signaling, role of BRCA1 in DNA damage response.

element-binding transcription factor 1 (SREBF1), a major regulator of lipid homeostasis, and FOXO4, a regulator of insulin signaling, were identified as significant transcription factors for cluster 2. Cluster 5 yielded transcription factors with well-known roles in the expression of liver-specific genes (HNF4a) and lipid homeostasis (PPARA and PPARD)[23,24].

Two clusters, 7 and 8, contained genes that were, respectively, decreased or increased at 12 h and 1 day PN compared to the other time points. Cholesterol synthesis and ethanol metabolism genes were identified for cluster 7 along with SREBF2, while canonical pathways associated with DNA repair and protein ubiquitination were identified for cluster 8. Associated transcription factors for cluster 8 genes included E2F family members, p53 and PPARA. Clusters 6 and 9 containing genes upregulated by 4 h through the rest of the time points and genes downregulated at 4 h PN compared to all other time points, respectively, did not result in significant canonical pathways or upstream regulators.

Pairwise Comparisons of Postnatal Expression Levels With E21 Fetal

In an approach meant to complement the previous temporal analysis, we identified those probesets that changed significantly between each PN time point and the E21 fetal samples (Fig. 3). There were no significant changes comparing E21 to 30 min PN. However, by 4 h PN, over 1,000 probesets showed a significant change from expression levels in the near-term E21 fetal samples. Additional changes were identified at all of the subsequent time points. There were differences in the magnitude of the fold change in gene expression at this earliest time point compared to the later PN samples. There was only one gene with a $\log_2$ fold change greater than 5 in the 4 h PN compared to E21 fetal sample, while there were over 10 genes in the 12 h PN compared to E21 fetal (Table 1). The expression of the majority of these genes was similar in the 1 day PN to E21 fetal comparison. At 7 days PN, 30 genes met this criteria compared to E21 fetal. The upregulated genes have functions (xenobiotic metabolism, nutrient transport, cell adhesion, and quiescence) associated with acquisition of a more mature hepatocyte phenotype, while downregulated genes were associated with a broader range of cellular functions, including proliferation, fatty acid biosynthesis, platelet aggregation, and hematopoiesis. To assess biological implications of these changes in gene expression, IPA was performed using all genes identified as significant (red dots in Fig. 3). Upregulated and downregulated genes were analyzed separately.

At 4 and 12 h PN, analysis of the upregulated genes yielded canonical pathways (Table 2) associated with inflammatory signaling (IL-6 signaling and acute phase reactants). No significant canonical pathways were identified using the downregulated genes at 4 h PN. Canonical pathways related to cholesterol biosynthesis were downregulated at 12 h and 1 day PN. At 7 days PN, canonical pathways identified by upregulated genes related to

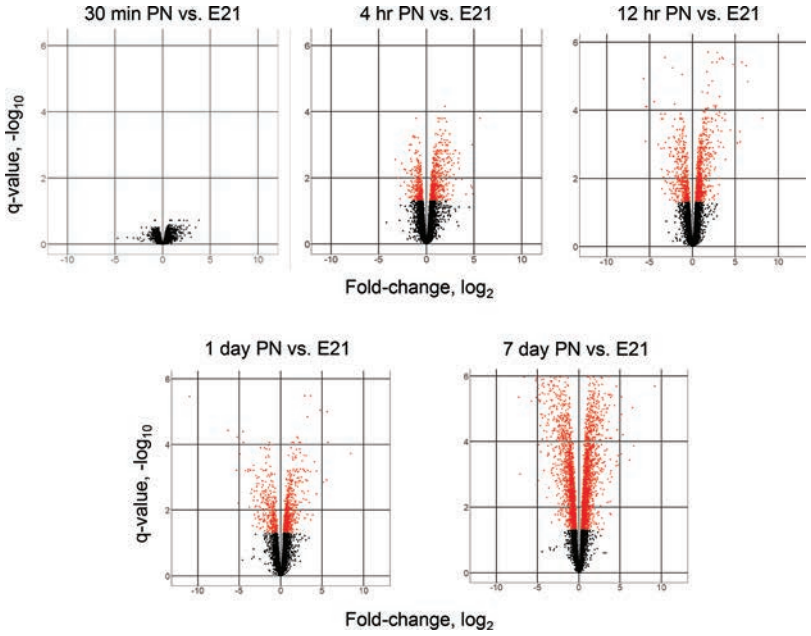

Figure 3. Volcano plots derived from pairwise comparisons of postnatal time points to fetal (E21). Gene expression is graphed as the negative $\log_{10}$ of the *q* value versus the $\log_2$ of the fold change (PN to E21 ratio) for all coding genes detected in the microarray analysis. Genes that showed a significant change [false discovery rate (FDR) < 0.05] are represented by the red dots.

Table 1. Significant Probesets With Log_2 Fold Change ±5 Comparing Postnatal Time Points to Fetal

4 h PN	12 h PN	1 Day PN	7 Days PN
Coq10b (+48.9; 0.0002)	Inhbe (+286.4; 0.0002)	Inhbe (+345; 0.0002)	Cyp1a2 (+587.2; 0.000002)
	Slc34a2 (+88.1; 0.00001)	Slc34a2 (+52.4; 0.00009)	Ces2e (+178.2; 0.00000001)
	Plin2 (+74.6; 0.000005)	Acot1 (+49.1; 0.00001)	Inhbe (+100.5; 0.0001)
	Acot1 (+53; 0.000004)	Cyp3a23/3a1 (+46.6; 0.001)	Ces1c (+90.2; 0.000009)
	Cyp3a23/3a1 (+47; 0.0008)	Cyp3a23/3a1 (+34.9; 0.001)	Cyp2c6v1 (+71.2; 0.0004)
	Slc25a47 (+45.6; 0.0004)	Hdc (−2080; 0.000003)	Car3 (+40.2; 0.00006)
	Cyp3a23/3a1 (+36.8; 0.0009)	Scd (−83.5; 0.00004)	Avpr1a (+35.5; 0.00001)
	Abhd2 (+31.9; 0.0000003)	Rbp2 (−40.3; 0.0006)	Slc13a4 (+35.5; 0.000004)
	Insig1 (−51.5; 0.00001)	Insig1 (−37.6; 0.00006)	RGD6491302_1 (+35.2; 0.0002)
	Hdc (−44.9; 0.0008)	Scd1 (−34.6; 0.006)	Slc34a2 (+31.9; 0.00002)
	Scd (−43.7; 0.00008)		Cldn3 (+31; 0.000001)
	LOC688922 (−40.5; 0.00008)		Hdc (−5790.8; 0.0000002)
			Rbp2 (−157.1; 0.000004)
			Cyp7a1 (−141; 0.001)
			Ppbp (−98.9; 0.000001)
			Gsn (−91.3; 0.0000007)
			Hif3a (−86.4; 0.0000004)
			Scd (−54.6; 0.000006)
			Pf4 (−50.4; 0.0000006)
			Gp9 (−43.5; 0.0000009)
			Ermap (−40.2; 0.0000004)
			Mpo (−37.8; 0.0000004)
			Spta1 (−37.6; 0.000001)
			Gp5 (−36.8; 0.0000006)
			Ca1 (−36.6; 0.000001)
			Gpc3 (−36.5; 0.000004)
			Lpin1 (−36.3; 0.000001)
			Serpinb10 (−32.6; 0.000001)
			Rhag (−31.4; 0.000002)
			Ahsp (−31.2; 0.000002)

Data are shown as gene symbol (fold change; *q* value) with directional change compared to E21 fetal.

cellular signaling and mature liver functions. Pathways related to cell cycle, mitosis, and ribosome biogenesis were identified as downregulated at 7 days PN.

The IPA results for transcription factors mirrored the results for canonical pathways (Fig. 4). Transcriptional regulators with roles in inflammation and cell stress, NFkB, STAT3, and FOXO3, were identified at 4 h PN (Fig. 4A). Genes downstream from CLOCK, ID2, and ID3, all of which are involved in circadian regulation of gene expression[25], were also increased at 4 h PN. No transcription factors were identified as specifically activating gene expression at E21 relative to 4 h PN.

There was significant overlap in the transcription factors identified when comparing 12 h and 1 day PN to E21 (Fig. 4B and C). Transcriptional regulators with roles in the expression of liver-specific genes and mature liver function (PPARA, PPARD, and HNF4A) were identified in the PN samples, while SREBF2, SREBF1, PPARA, FOXO4, and RORA were associated with genes downregulated in these PN samples compared to E21 fetal. Using Cytoscape to visualize the overlap in genes that account for the identification of transcription factors in the 12 h and 1 day PN comparison to E21 (Fig. 4D), we found that at least 50% of the genes associated with PPARA, PPARD, and HNF4A overlapped at 12 h and 1 day PN. Similar overlap was observed in the genes accounting for identification of significant transcriptional regulators associated with genes downregulated at 12 h and 1 day PN compared to E21. There was no overlap in the PPARA targets between the PN and E21 time points. At 7 days PN, upregulated genes identified many transcription factors related to the mature hepatocyte phenotype, while genes decreased on day 7 PN compared to E21 identified transcription factors related to cell cycle and hematopoiesis.

Gene Set Enrichment Analysis

We used GSEA[19] to examine the relative enrichment of functionally related gene sets among all probesets detected by the microarray. This allows for the

Table 2. Ingenuity Pathway Analysis (IPA) Comparing Postnatal Time Points to Fetal (E21)

Comparison	Gene Expression Relative to E21	IPA Canonical Pathways (p Value $<10^{-7}$)	Representative Genes
E21 to 4 h PN	Upregulated	Il-6 signaling	Cytokine receptors, MAPK family members
	Downregulated	None	N/A
E21 to 12 h PN	Upregulated	IL-6 signaling, acute phase reactants	Cytokine receptors, TNF receptor family, MAPK family members
	Downregulated	Superpathway of cholesterol biosynthesis, cholesterol biosynthesis, cholesterol biosyntheses II and III, ethanol degradation	Cholesterol synthesis genes (DHCR24, HMGCR,LSS), aldehyde dehydrogenases, acyl-CoA synthetases
E21 to 1 day PN	Upregulated	None	N/A
	Downregulated	Superpathway of cholesterol biosynthesis, cholesterol biosynthesis I, cholesterol biosyntheses II and III	Cholesterol synthesis genes (DHCR24, HMGCR,LSS)
E21 to 7 days PN	Upregulated	Regulation of the epithelial–mesenchymal transition pathway	Growth factor receptors
		STAT3 pathway, hepatic fibrosis/hepatic stellate cell activation, acute phase response signaling, PTEN signaling, molecular mechanisms of cancer, colorectal cancer metastasis signaling, xenobiotic metabolism signaling, FXR/RXR activation, LXR/RXR activation, Paxillin signaling, integrin signaling, IL-8 signaling, mouse embryonic stem cell pluripotency	MAPK family members, collagens, interleukins, receptor tyrosine kinases, Cyp450s, adhesion molecules (ITGA8, ITGA9)
		Regulation of the epithelial–mesenchymal transition pathway	Growth factor receptors
	Downregulated	EIF2 signaling, cell cycle control of chromosomal replication, regulation of eIF4 and p70SK signaling, cell cycle: G_1/S checkpoint regulation, mitotic roles of Polo-like, mTOR signaling, cell cycle: G_2/M DNA damage checkpoint regulation	Ribosomal proteins, translation initiation factors, cyclins, mini-chromosome maintenance complex members, Polo-like kinases, 14-3-3 family members

identification of numerous small differences in gene expression that impact the same functional pathway. Results supported the findings obtained using IPA. While there were no individual genes that were statistically significant comparing the E21 fetal and 30 min PN time points, several Reactome gene sets were identified as highly significant. Fetal samples were enriched in pathways related to branched chain amino acid metabolism, the TCA cycle, respiratory electron transport, and fatty acid -oxidation. At 30 min PN, similar to the IPA results, there was enrichment of pathways related to inflammation and circadian functions. Genes associated with fatty acid -oxidation were enriched in fetal samples relative to the 4 h PN samples, while the latter showed enrichment of pathways related to protein translation relative to the near-term fetal time point.

By 12 h of life, multiple pathways related to the cell cycle were enriched relative to fetal samples. GSEA also indicated a decreased expression of genes related to cholesterol synthesis at 12 h PN. Similar results were seen at the 1 day PN time point. By 7 days PN, pathways reflecting cell cycle activity were downregulated.

GSEA results for transcription factor targets were further examined using Cytoscape (Fig. 5). For this analysis, transcription factor targets whose gene sets overlapped by at least 95% are shown as connected by a line. At 30 min PN, numerous individual transcription factor targets related to inflammation and oxidative stress, including STAT proteins, NFKB, ATF3, HIF1, and CREBP1, were enriched relative to E21. Enrichment of many of these targets persisted at 4 h PN, with several transcription factor pathways showing considerable overlap (CREBP1CJUN_01, TGACCTTG_SF1_Q6, CREB_01 and TGACCTY_ERR1_Q2). At 1 day PN, all the significant transcription factor target gene sets that were enriched relative to E21 related to E2F-mediated signaling, suggesting a change in cell cycle activity. There were no significant transcription factor targets enriched in the E21 samples compared to 30 min, 4 h, or 1 day PN. By 7 days PN, E2F-related transcription factors were

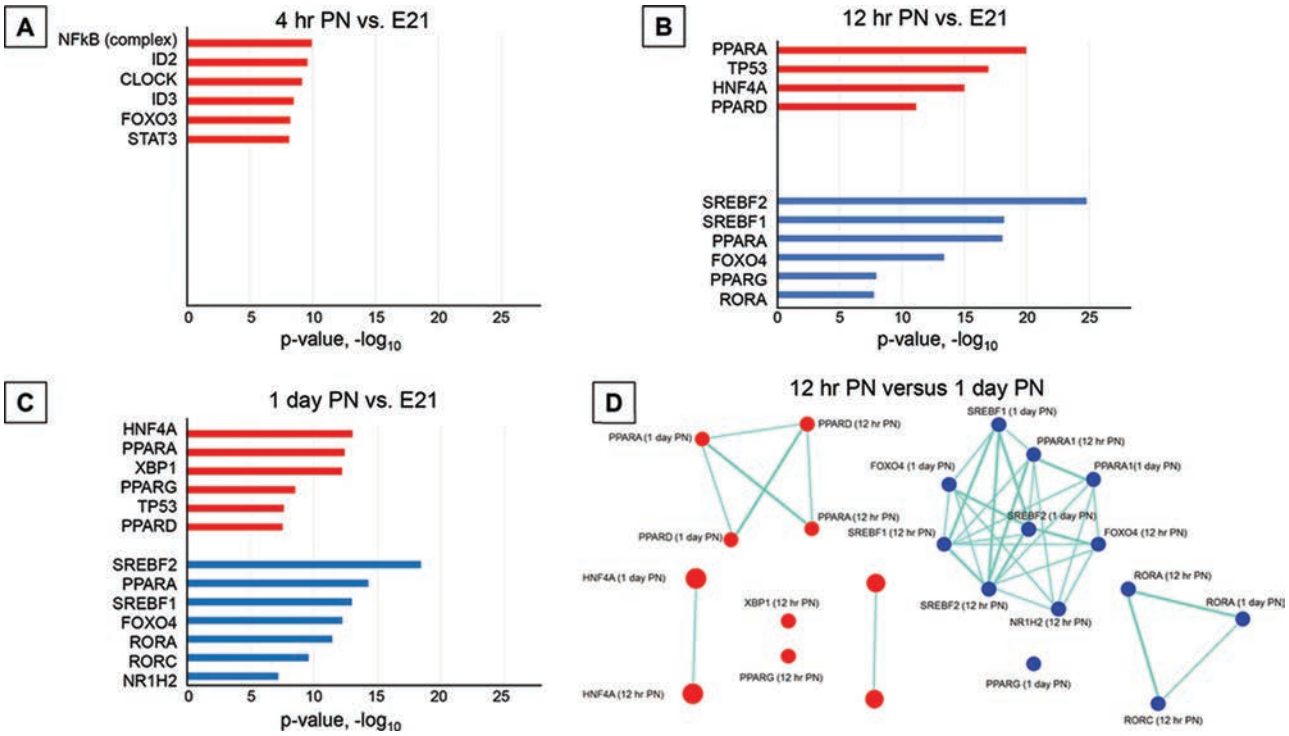

Figure 4. Significant transcription factors ($p < 10^{-7}$) identified by IPA of differentially expressed genes (FDR < 0.05) in pairwise comparisons of postnatal time points to fetal (E21). (A) 4 h PN versus E21. (B) 12 h PN versus 21. (C) 1 day PN versus E21. Red bars represent significant transcription factors identified in postnatal samples, and blue bars represent transcription factors identified in E21 samples. **(**D) Depiction of the overlap in genes accounting for the identification of specific transcription factors comparing the 12 h and 1 day PN samples assessed using Cytoscape. Lines connect nodes when 50% of the genes are in common. The thickness of the line increases with increasing percentage of overlap. Node size correlates with the number of gene targets for a particular transcription factor. Red nodes indicate transcription factors identified by genes whose expression was upregulated at 12 h or 1 day PN relative to E21. Blue nodes indicate transcription factors identified by genes whose expression was downregulated at 12 h or 1 day PN relative to E21.

enriched in the E21 sample, while no transcription factors were identified as enriched at 7 days PN.

Mitochondrial Gene Expression

Given the marked changes in metabolism that occur in the perinatal period[26] and the critical role of mitochondria in intermediary metabolism, we focused on changes in nuclear-encoded mitochondrial genes. Genes included in MitoCarta, a database of 1,158 genes with strong evidence of mitochondrial localization, were extracted from our microarray and analyzed by ANOVA. About half of these mitochondrial genes changed significantly across our full time course with approximately a quarter changing in the first day.

Temporal clustering of the significant mitochondrial genes resulted in three clusters with a sufficient number of genes (>100) to perform IPA (Fig. 6). Cluster 1, containing genes upregulated at 7 days PN, was associated with tryptophan degradation. Genes whose expression was upregulated between 4 and 12 h PN (cluster 2) were related to fatty acid -oxidation and were downstream of PPARA, PPARD, and KLF15. Cluster 3, containing genes downregulated at 7 days PN, was associated with the TCA cycle and contained numerous c-Myc targets.

Assessment of Specific Metabolic Pathways

Gene sets identified using PathCards were used to focus on selected pathways we viewed as highly relevant to perinatal changes in intermediary metabolism. Each individual pathway was used to construct a separate heat map (Fig. 7). The mean expression for each gene in the pathway for individual PN time points was compared to fetal samples. The relative change in expression is reflected by the colors of the heat maps.

The glycolysis heat map showed a preponderant downregulation at 7 days PN of the expression of genes that encode key glycolytic enzymes. The regulatory subunits for protein phosphatase 2A (designated as "Ppp2__") were induced at or around the 12 h PN time point. Gluconeogenesis showed coordinated upregulation at 12 h PN of Slc25a genes, which encode carriers that are required for transport of metabolic intermediates across mitochondrial membranes[27].

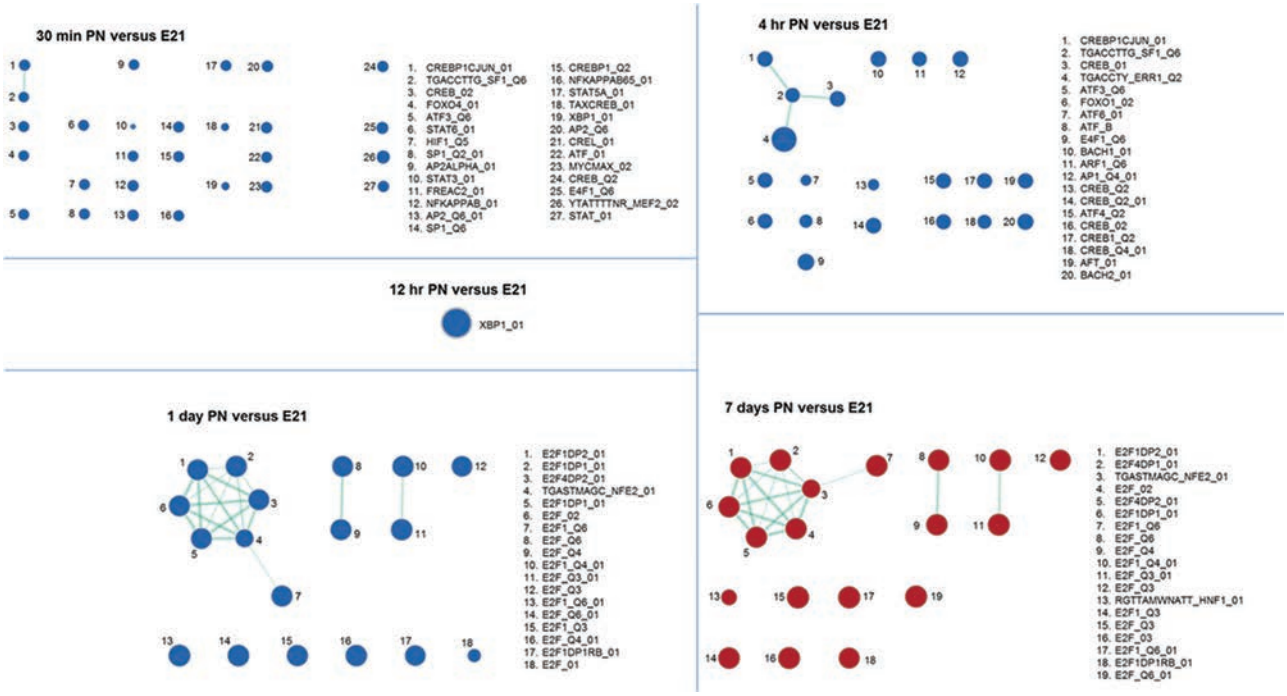

Figure 5. Transcription factor targets identified by gene set enrichment analysis (GSEA) and depicted using Cytoscape. Transcription factor targets identified as significant ($q < 0.005$) by GSEA in comparisons of postnatal time points to the fetal (E21) time point were entered in Cytoscape. Nodes represent individual transcription factor target datasets. Lines connect nodes when 95% of genes are in common between the two nodes. Nodes shown in red represent candidate transcriptional regulators whose targets were enriched in the postnatal samples. Blue nodes indicate regulators of gene sets whose targets were enriched in the E21 samples relative to a given postnatal time point. The relative size of nodes is related to the number of genes associated with the transcription factor target, and the line weight connecting nodes is related to the overlap between the nodes.

The gene sets representing glycogen metabolism showed no obvious temporal pattern. However, our laboratory showed previously that the enzymes directly involved in glycogen metabolism (assessed by measuring enzyme activity) are gradually induced in the fetal rat starting on day 17[28]. These earlier studies indicate that the induction of these genes likely occurred prior to our earliest PN time point.

Examination of a gene set representing fatty acyl-CoA synthesis showed coordinated induction of acyl-CoA thioesterases (Acot__) at 12 h PN, while acyl-CoA synthases (Acs__) were generally induced only at 7 days PN. However, two enzymes that are rate limiting for fatty acid synthesis, ATP-citrate lyase (Acly), and fatty acid synthase (FASN) showed marked downregulation at 4–12 h PN. The fatty acid -oxidation gene set, on the other hand, showed several genes with increased expression at or before 1 day PN.

In terms of cholesterol biosynthesis, there was a notable decrease at 12 h PN in expression of INSIG1, which is a key regulatory enzyme for cholesterol synthesis. Members of the SEC23/SEC24 family, which are involved in vesicle trafficking, were induced at 12 h.

Neither TCA, urea cycle genes, nor genes encoding components of the respiratory chain, including NADH: ubiquinone oxidoreductase subunits (Nduf__) and ATP synthase subunits (Atp__), showed coordinated regulation.

DISCUSSION

Around birth, mammalian newborns are subject to a host of physiologic stressors to which they must adapt[29]. Among the most profound changes that occur during the transition from in utero to extrauterine life is the rise in oxygenation associated with breathing ambient air, a change that results in significant oxidative stress[30]. Newborns respond to cold stress by activating brown adipose tissue thermogenesis[31]. With regard to nutrient supply, the perinatal period sees a transition from a constant infusion of carbohydrate-predominant nutrition via the placenta to intermittent feeds with a lipid-enriched nutrient supply[32,33]. These nutritional changes coincide with a shift in the hormone milieu from a high-insulin/low-glucagon state in utero to low-insulin/high-glucagon postbirth, which transiently shifts metabolism from an

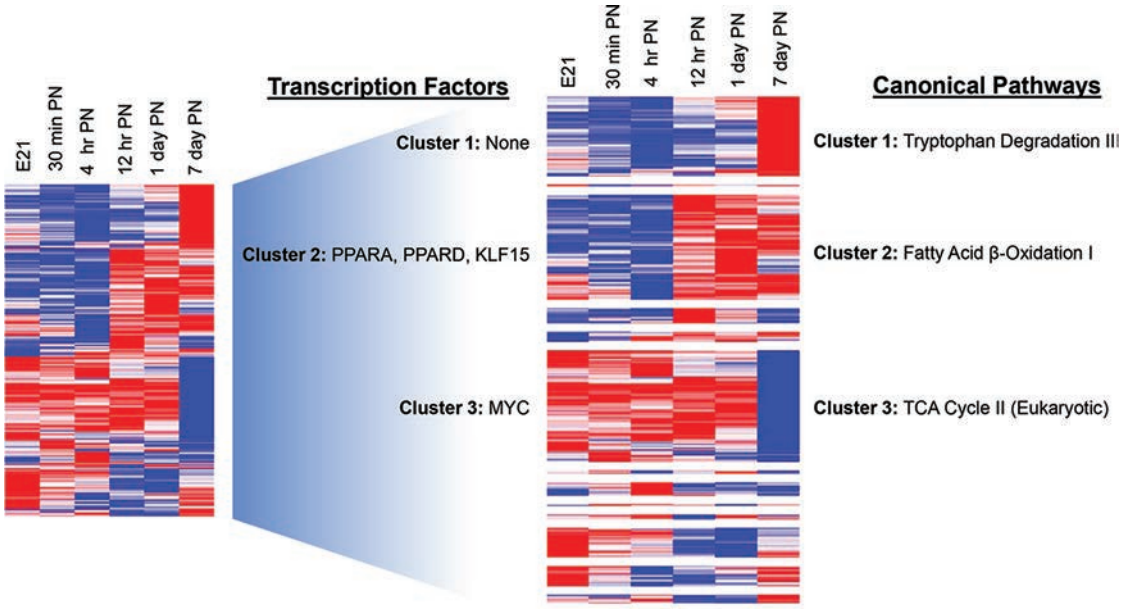

Figure 6. Cluster analysis of the temporal pattern of mitochondrial gene expression. Significant genes ($q < 0.05$) contained in MitoCarta, a compendium of 1,158 nuclear genes related to mitochondria, were extracted from the dataset. The mitochondrial genes were then separated into clusters based on temporal expression patterns. Clusters with greater than 100 genes were entered into IPA. Of these, three clusters were associated with significant canonical pathways and upstream regulators. The heat map colors represent the relative expression level, with blue corresponding to the lowest level across a row and red corresponding to the highest expression in that row.

anabolic to a catabolic state[2]. This transition is also associated with a rise in catecholamines during and just after parturition[34].

Given the significant role of the liver in the perinatal metabolic transition[26], several studies have profiled the transcriptome during this period[35–37]; these studies did not examine events in the immediate PN period. Two of these studies evaluated perinatal changes in the liver transcriptome in rodent models. Chapple et al.[35] used RNA-Seq to examine changes in gene expression in the rat across a broad developmental time frame from early gestation (embryonic day 14) to PN days 1 and 7. They found enrichment of gene expression relating to mitochondrial metabolism and cholesterol synthesis. Their analysis did not include identification of common regulatory elements across the differentially expressed genes. Gunewardena et al.[36], also using RNA-Seq, examined changes in hepatic gene expression in mice. These authors focused on a single late embryonic time point, 2 days before birth, and PN time points extending to 60 days after birth. They found that over 7,000 genes were differentially regulated with age and that over 800 had multiple splice variants. These researchers queried upstream regulators; however, neither study focused on the first 24 h of PN life. A third study by Li et al.[37] used microarray analysis to study circadian rhythm-related genes in a two-way comparison of late gestation fetal and adult mouse livers. While these investigators observed a key distinction between the circadian oscillators in fetal and adult liver, perinatal gene expression was not a focus of their work.

We found that the most marked change in hepatic gene expression occurred not at the earliest time points, 30 min or 4 h PN, but during the period between 4 and 12 h PN. This transition appears to involve oxidative stress and increased cytokine signaling at 4 h PN. This, in turn, can account for activation of various cell signaling pathways (cAMP-mediated signaling, Ras–MAPK, and AP-1) that result in changes in cell adhesion and metabolism and ultimately promote differentiation through the activation of transcription factors with well-known roles in the expression of liver-specific genes, xenobiotic metabolism, and intermediary metabolism.

A limitation of the current study is that the nutritional status of the individual pups was not controlled. Pups harvested at 30 min did not have a milk spot, and visualization of the stomach showed no milk. However, by 4 h PN, all pups had visible milk in their stomachs, and this trend continued through 7 days PN. We cannot rule out the subtle differences in fed state may account for some of the changes in gene expression.

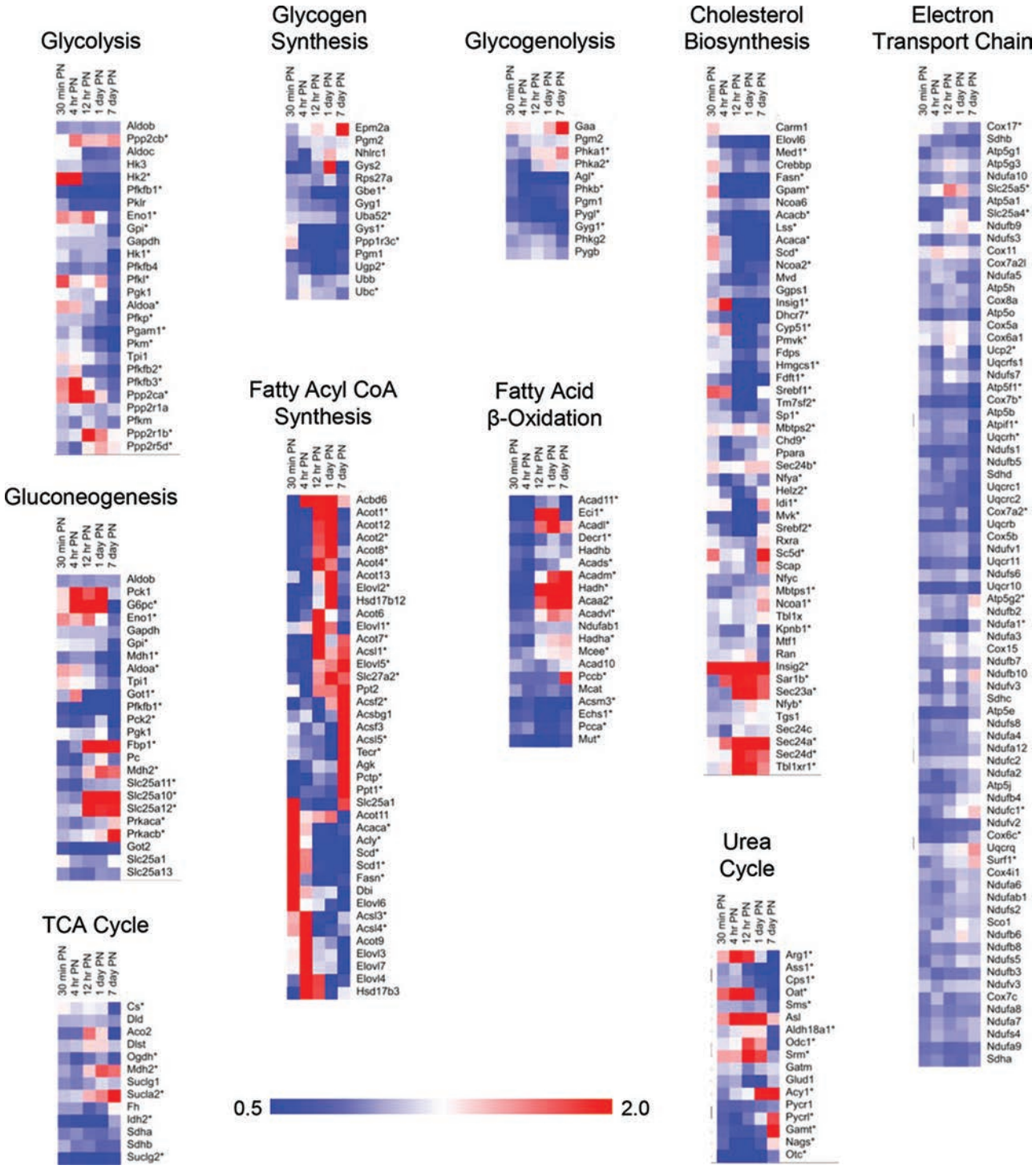

Figure 7. Heat maps of select metabolic pathways. Genes associated with select metabolic pathways were extracted from PathCards, and heat maps were created. The mean expression for each gene in the pathway for individual postnatal time points was normalized to the mean of the E21 fetal samples. The relative change in expression is reflected by the colors of the heat maps. *Genes that changed significantly ($q < 0.05$). Genes are clustered by row.

Changes in nutrient composition and the transition to intermittent feeds may contribute to many of the changes in gene expression seen through 12 h PN. With regard to cholesterol metabolism, the peak in HMG-CoA reductase, the rate-limiting enzyme for cholesterol synthesis, just before birth, and its decrease during the first PN day have been attributed to the dietary intake of cholesterol in breast milk[4,38]. Our expression data showed broader effects of this transition that included other enzymes and transporters.

Our lab showed previously that hepatocyte proliferation in the rat wanes during the 2 days before birth but then resumes in a synchronous manner starting on the first PN day[39]. Hepatocytes transition to a quiescent state by the end of the first PN week. In the present studies, we observed enrichment of genes related to cell proliferation by 1 day PN. By 7 days PN, genes related to proliferation were downregulated. In addition, there was enrichment at 7 days PN of numerous pathways consistent with a more mature hepatic phenotype as reflected by genes involved in xenobiotic metabolism and extracellular signaling.

An unexpected finding was the high proportion of mitochondrial genes that changed significantly in the immediate PN period. Our work agrees with the established observation[15] that at birth hepatocytes have high levels of mRNA encoding mitochondrial proteins, which are then translated after birth. Prebirth, there are relatively fewer, large mitochondria with decreased capacity for aerobic ATP synthesis and decreased capacity for gluconeogenesis, ureagenesis, and fatty acid oxidation[5]. Post-birth, there is rapid maturation of mitochondria, which is largely controlled at the mRNA translation level[40]. However, there is also a neonatal increase in mitochondrial mass, which involves both transcriptional and posttranscriptional mechanisms that support mitochondrial biogenesis[15]. Much like tumor cells, fetal hepatocytes rely more on glycolysis than oxidative phosphorylation for energy production[41]. This latter point is reflected in our data showing the changes in gene expression for glycolysis-related genes. We speculate that the rise and fall in enrichment of glycolysis genes are associated with the transient period of hepatocyte proliferation, which slows by the end of the first PN week.

Our data may be viewed in relation to the phenomenon termed "hormesis"[42], which refers to the beneficial effects that result from exposure to a low level of an instigating agent or stimulus that is toxic when present at a higher level. An example of this is the mitigation of injury that occurs when brief periods of hypoxia precede experimental myocardial infarction[43]. This concept has also been established for liver in the context of preconditioning liver tissue to improve resistance to the ischemia–reperfusion injury associated with liver transplantation[44]. During the perinatal transition, the neonate is exposed to stressors that can induce injury, but that may also lead to greater tolerance to the rapid and marked environmental changes to which the newborn is subjected. Our studies are a first step in identifying mechanisms that mediate changes in gene expression during the perinatal transition, any of which could represent targets for interventions aimed at improving neonatal outcomes.

ACKNOWLEDGMENTS: The authors thank Dr. Christoph Schorl of Brown University's Center for Genomics and Proteomics for performance of the microarrays. These studies were supported by the National Institutes of Health grant R01HD024455 (P.A.G. and J.A.S.) and by the Rhode Island Hospital Department of Pediatrics. Valerie Zabala is a Howard Hughes Medical Institute Gilliam Fellow. The authors declare no conflicts of interest.

REFERENCES

1. Gonzalez MM, Madrid R, Arahuetes RM. Physiological changes in antioxidant defences in fetal and neonatal rat liver. Reprod Fertil Dev. 1995;7(5):1375–80.
2. Girard JR, Cuendet GS, Marliss EB, Kervran A, Rieutort M, Assan R. Fuels, hormones, and liver metabolism at term and during the early postnatal period in the rat. J Clin Invest. 1973;52(12):3190–200.
3. Asikainen TM, Raivio KO, Saksela M, Kinnula VL. Expression and developmental profile of antioxidant enzymes in human lung and liver. Am J Respi Cell Mol Biol. 1998;19(6):942–9.
4. Haave NC, Innis SM. Cholesterol synthesis and accretion within various tissues of the fetal and neonatal rat. Metabolism 2001;50(1):12–8.
5. Valcarce C, Navarrete RM, Encabo P, Loeches E, Satrustegui J, Cuezva JM. Postnatal development of rat liver mitochondrial functions. The roles of protein synthesis and of adenine nucleotides. J Biol Chem. 1988;263(16):7767–75.
6. Mayor F, Cuezva JM. Hormonal and metabolic changes in the perinatal period. Biol Neonate 1985;48(4):185–96.
7. Greengard O. Enzymic differentiation in mammalian liver injection of fetal rats with hormones causes the premature formation of liver enzymes. Science 1969;163(3870):891–5.
8. Moscovitz JE, Aleksunes LM. Establishment of metabolism and transport pathways in the rodent and human fetal liver. Int J Mol Sci. 2013;14(12):23801–27.
9. Gruppuso PA, Sanders JA. Regulation of liver development: Implications for liver biology across the lifespan. J Mol Endocrinol. 2016;56(3):R115–25.
10. Boylan JM, Anand P, Gruppuso PA. Ribosomal protein S6 phosphorylation and function during late gestation liver development in the rat. J Biol Chem. 2001;276:44457–63.
11. Anand P, Boylan JM, Ou Y, Gruppuso PA. Insulin signaling during perinatal liver development in the rat. Am J Physiol Endocrinol Metab. 2002;283(4):E844–52.
12. Boylan JM, Gruppuso PA. Uncoupling of hepatic, epidermal growth factor-mediated mitogen-activated protein kinase activation in the fetal rat. J Biol Chem. 1998;273:3784–90.
13. Gruppuso PA, Awad M, Bienieki TC, Boylan JM, Fernando S, Faris RA. Modulation of mitogen-independent hepatocyte proliferation during the perinatal period in the rat. In Vitro Cell Dev Biol Animal 1997;33(7):562–8.
14. Aprille JR. Perinatal development of liver mitochondrial function. In: Cuezva JM, Pascual-Leone AM, Patel MS,

editors. Endocrine and biochemical development of the fetus and neonate. Boston (MA): Springer; 1990. p. 101–12.
15. Cuezva JM, Ostronoff LK, Ricart J, Lopez de Heredia M, Di Liegro CM, Izquierdo JM. Mitochondrial biogenesis in the liver during development and oncogenesis. J Bioenerg Biomembr. 1997;29(4):365–77.
16. Adebayo Michael AO, Ahsan N, Zabala V, Francois-Vaughan H, Post S, Brilliant KE, Salomon AR, Sanders JA, Gruppuso PA. Proteomic analysis of laser capture microdissected focal lesions in a rat model of progenitor marker-positive hepatocellular carcinoma. Oncotarget 2017;8(16): 26041–56.
17. Gentleman R, Carey V, Huber W, Hahne F. Genefilter: Methods for filtering genes from high-throughput experiments. R package version 1.60.0 [Internet]. 2017 [cited June 2018]. Available from https://bioconductor.org/packages/release/bioc/html/genefilter.html
18. Lamming DW, Demirkan G, Boylan JM, Mihaylova MM, Peng T, Ferreira J, Neretti N, Salomon A, Sabatini DM, Gruppuso PA. Hepatic signaling by the mechanistic target of rapamycin complex 2 (mTORC2). FASEB J. 2014; 28(1):300–15.
19. Subramanian A, Kuehn H, Gould J, Tamayo P, Mesirov JP. GSEA-P: A desktop application for Gene Set Enrichment Analysis. Bioinformatics 2007;23(23):3251–3.
20. Shannon P, Markiel A, Ozier O, Baliga NS, Wang JT, Ramage D, Amin N, Schwikowski B, Ideker T. Cytoscape: A software environment for integrated models of biomolecular interaction networks. Genome Res. 2003;13(11): 2498–504.
21. Calvo SE, Clauser KR, Mootha VK. MitoCarta2.0: An updated inventory of mammalian mitochondrial proteins. Nucleic Acids Res. 2016;44(D1):D1251–7.
22. Belinky F, Nativ N, Stelzer G, Zimmerman S, Iny Stein T, Safran M, Lancet D. PathCards: Multi-source consolidation of human biological pathways. Database (Oxford) 2015. 2015.
23. Tyagi S, Gupta P, Saini AS, Kaushal C, Sharma S. The peroxisome proliferator-activated receptor: A family of nuclear receptors role in various diseases. J Adv Pharm Technol Res. 2011;2(4):236–40.
24. Babeu JP, Boudreau F. Hepatocyte nuclear factor 4-alpha involvement in liver and intestinal inflammatory networks. World J Gastroenterol. 2014;20(1):22–30.
25. Reinke H, Asher G. Circadian clock control of liver metabolic functions. Gastroenterology 2016;150(3):574–80.
26. Beath SV. Hepatic function and physiology in the newborn. Semin Neonatol. 2003;8(5):337–46.
27. Palmieri F. The mitochondrial transporter family SLC25: Identification, properties and physiopathology. Mol Aspects Med. 2013;34(2–3):465–84.
28. Gruppuso PA, Brautigan DL. Induction of hepatic glycogenesis in the fetal rat. Am J Physiol Endocrinol Metab. 1989;256(1 Pt 1):E49–54.
29. Hillman NH, Kallapur SG, Jobe AH. Physiology of transition from intrauterine to extrauterine life. Clin Perinatol. 2012;39(4):769–83.
30. Torres-Cuevas I, Parra-Llorca A, Sanchez-Illana A, Nunez-Ramiro A, Kuligowski J, Chafer-Pericas C, Cernada M, Escobar J, Vento M. Oxygen and oxidative stress in the perinatal period. Redox Biol. 2017;12:674–81.
31. Power G, Blood A. Thermoregulation. In: Polin RA, Fox WW, Abham SH, editors. Fetal and neonatal physiology. Philadelphia (PA): Elseveir; 2011. p. 615–24.
32. Kennaugh JM, Hay WW Jr. Nutrition of the fetus and newborn. West J Med. 1987;147(4):435–48.
33. Ballard O, Morrow AL. Human milk composition: Nutrients and bioactive factors. Pediatr Clin North Am. 2013;60(1):49–74.
34. Sperling MA, Ganguli S, Leslie N, Landt K. Fetal-perinatal catecholamine secretion: Role in perinatal glucose homeostasis. Am J Physiol. 1984;247(1 Pt 1):E69–74.
35. Chapple RH, Tizioto PC, Wells KD, Givan SA, Kim J, McKay SD, Schnabel RD, Taylor JF. Characterization of the rat developmental liver transcriptome. Physiol Genomics 2013;45(8):301–11.
36. Gunewardena SS, Yoo B, Peng L, Lu H, Zhong X, Klaassen CD, Cui JY. Deciphering the developmental dynamics of the mouse liver transcriptome. PLoS One 2015;10(10):e0141220.
37. Li C, Yu S, Zhong X, Wu J, Li X. Transcriptome comparison between fetal and adult mouse livers: Implications for circadian clock mechanisms. PLoS One 2012;7(2):e31292.
38. Haave NC, Innis SM. Perinatal development of hepatic cholesterol synthesis in the rat. Biochim Biophys Acta 1991;1085(1):35–44.
39. Curran TR Jr, Bahner RI Jr, Oh W, Gruppuso PA. Mitogen-independent DNA synthesis by fetal rat hepatocytes in primary culture. Exp Cell Res. 1993;209(1):53–7.
40. Izquierdo JM, Luis AM, Cuezva JM. Postnatal mitochondrial differentiation in rat liver. Regulation by thyroid hormones of the beta-subunit of the mitochondrial F1-ATPase complex. J Biol Chem. 1990;265(16):9090–7.
41. Gaull GE, Hommes FA, Roux JF. Human biochemical development. In: Falkner F, editor. Principles and prenatal growth. New York: Springer; 1978. p. 23–124.
42. Calabrese EJ, Bachmann KA, Bailer AJ, Bolger PM, Borak J, Cai L, Cedergreen N, Cherian MG, Chiueh CC, Clarkson TW; and others. Biological stress response terminology: Integrating the concepts of adaptive response and preconditioning stress within a hormetic dose-response framework. Toxicol App Pharmacol. 2007;222(1):122–8.
43. Murry CE, Jennings RB, Reimer KA. Preconditioning with ischemia: A delay of lethal cell injury in ischemic myocardium. Circulation 1986;74(5):1124–36.
44. Liu A, Fang H, Wei W, Dirsch O, Dahmen U. Ischemic preconditioning protects against liver ischemia/reperfusion injury via heme oxygenase-1-mediated autophagy. Crit Care Med. 2014;42(12):e762–71.